

## Supplemental Materials

### Key interactions in the trimolecular complex consisting of the rheumatoid arthritis-associated DRB1\*04:01 molecule, the major glycosylated collagen II peptide, and the T-cell receptor

#### MATERIALS AND METHODS

##### Peptide synthesis

Unmodified human Col2<sub>259-273</sub> (GIAGFKGEQGPKGET); mutated Col2<sub>259-273</sub> (GIAGFAGEQGPAGEP, HA (hemagglutinin)<sub>306-318</sub> (PKYVKQNTLKLAT); and citrullinated CILP(cartilage intermediate layer protein)<sub>982-996</sub> (GKLYGI(Cit)DV(Cit)STRDR) were synthesized by Biomatik Corporation. The glycopeptide gal<sub>264</sub>Col2<sub>259-273</sub> (GIAGFK-GalGEQGPKGET) was synthesized using a procedure reported previously.[1] Purity of each peptide was >95%. All peptides were dissolved in phosphate-buffered saline at a concentration of 10 mg/ml and kept frozen at -20°C for further use. The gal building blocks were synthesized by Taros Chemicals (Dortmund, Germany).[1]

##### Production of the recombinant MHCII/peptide complexes

The DRB1\*04:01/hCLIPmut molecules were designed according to Gauthier et al. [2] with modification. The native leader sequences of the  $\alpha$ - and  $\beta$ -chains were replaced by a *Drosophila* BiP protein signal sequence. The extracellular domains of DRB1\*04:01 were truncated and the transmembrane regions were replaced by an acidic and basic zipper dimerization motif, respectively. A low affinity peptide hCLIPmut (PVSKARMATGALAQA) followed by a thrombin cleavage site was covalently linked to the

N-terminus of the  $\beta$  chain. In addition, C-terminal of the  $\alpha$ -chain, a 15 amino acid AviTag peptide for site-specific biotinylation was inserted after the basic zipper whereas a polyhistidine tag was attached C-terminal of the  $\beta$ -chain following an interposed acidic zipper.

The genes were synthesized at Eurofins with *KpnI* and *XhoI* restriction sites at the 5' and 3' ends. The synthesized genes were digested by restriction enzymes using FastDigest™ enzymes (ThermoFisher Scientific). The digested DNA fragments were cloned into a mammalian expression vector pCEP4 (Life Technologies) that was digested using the same restriction enzymes. After sequence verification, the recombinant plasmids were co-transfected into Expi393F™ cells (Life Technologies) with FectoPRO™ DNA transfection reagent (Polyplus transfection). The supernatants were harvested 6 days post transfection. The recombinant protein was first captured using a 5 mL HisTrap Excel (GE Healthcare Life Sciences) affinity column followed by size exclusion chromatography on Superdex 200 pg (GE Healthcare Life Sciences). The recombinant protein was purified as a single peak and concentrated by diafiltration into 20 mM Tris-HCl, 50 mM NaCl, pH 8.0 buffer using an Amicon centrifuge device with MWCO of 10 kDa. For biotinylation, incubation with biotin-protein ligase was carried out according to the manufacturers' instruction (Avidity, Denver, CO) at 30°C for 2 hours. Cleavage by thrombin (Novagen, 1 unit thrombin to 1 mg purified protein) to remove the covalently linked hCLIPmut peptide and its replacement by incubation with a desired peptide in excess was performed to generate well-defined MHCII complexes with different peptide loads. The reaction mixture was incubated at ambient temperature overnight with slow rotation followed by incubation at 4°C for 2 days. Cleaved hCLIPmut, excess of peptide, free biotin, were removed by size exclusion chromatography on a Superdex 200 pg column.

### **Flow cytometric detection of human Col2-specific T cells in peripheral blood**

For flow cytometric detection of antigen specific CD4<sup>+</sup> T cells, fluorochrome-labelled DRB1\*04:01 Col2-peptide tetramer complexes were generated. The biotinylated recombinant DRB1\*04:01 molecules were loaded with either the unmodified synthetic Col2 peptide 259-271 (nCol2) or its variant containing a galactose attached to the hydroxylated lysine residue at position 264 (gal<sub>264</sub>Col2). Subsequently, the monomeric complexes were incubated as a fourfold molar excess with either phycoerytherin (PE) or allophycocyanin labeled streptavidin molecules (Life Technologies, Sigma, BioLegend) for 1 hour at 37°C for fluorescence labelling and tetramerization.

The analysis for the detection of Col2-specific T lymphocytes was performed on the CD4-enriched fraction (CD4 T cell isolation kit, Miltenyi Biotec) of peripheral blood mononuclear cells (PBMC) prepared from whole blood samples of human donors. For staining, 1 x 10<sup>6</sup> cells/mL CD4<sup>+</sup> T cells were incubated with 2 µl Fc receptor blocking reagent (Human FC block, Miltenyi Biotec #130-059-901) and 1 µl dasatinib (50 nM final concentration) to prevent T-cell receptor downregulation by internalization. Subsequently the cells were stained with a FITC-conjugated anti-CD4 antibody (BB515FITC,#564418; BD, San Jose, CA) and either fluorescent streptavidin/biotin control conjugates (negative control) or DRB1\*04:01-tetramer complexes (DRB1\*04:01/gal<sub>264</sub>Col2 or DRB1\*04:01/nCol2) by incubation at a concentration of 20 µg/ml in 100 µl for 1h at 37° C. The CD4<sup>+</sup> T cells were then analyzed for DRB1\*04:01/Col2 peptide tetramer and negative control conjugate binding by flow cytometry (FACS Fortessa [BD; Franklin Lakes, NJ], FlowJo Software [Treestar; Ashland, OR]) gating on the CD4<sup>+</sup> cells in the live population according to live/dead marker (Zombie NIR, Biolegend #77184) staining. Statistical calculation of the percentage of RA patients and healthy donors (HDs) who had Col2-specific T cells above the negative control was based on the assumption of streptavidin/biotin tetramer staining representing background

resulting from unspecific binding. As occurrences of nonspecific streptavidin/biotin tetramer binding should be independent of the individual and the health condition, all streptavidin/biotin tetramer values from RA patients and HDs were averaged and the standard deviation was calculated. The threshold of positivity was set as the mean value of the background topped up with the threefold value of the standard deviation. Any individual with a raw TTS+ (positive tetramer staining) values above the threshold of positivity counted as positive.

*TTS + value of a positive individual > threshold of positivity*

$$\text{threshold of positivity} = \frac{\sum \text{Biotin TTS} + (\text{from all RA and HD})}{\text{total number of RA and HD}} + 3 \times \text{Standard deviation}$$

$$\text{percentage of positive RA patients} = \frac{\text{number of RA patients above threshold}}{\text{total number of RA patients}} \times 100$$

$$\text{percentage of positive HD} = \frac{\text{number of HD above threshold}}{\text{total number of HD}} \times 100$$

The values depicted in Figure 3B represent processed data in which for each tetramer staining datapoint the respective biotin background has already been subtracted from the raw value.

In addition, an activation assay of Col2 peptide specific to CD4<sup>+</sup> T cells in HLA-DRB1\*04:01 RA patients was performed by the stimulation of PBMCs with either synthetic galCol2 or nCol2 peptides for 7 h. The subsequent flow cytometric detection of surface staining for the T cell activation marker CD154 (CD40L) allowed quantification of stimulus dependent upregulation compared to buffer incubated negative control. The strong upregulation of CD154 on the CD4<sup>+</sup> T-cell population surface expression in response to superantigen SEB stimulation served as a positive control and criterion for inclusion of the respective Col2 peptide induced activation measures for further statistical analysis.

All blood sample donors gave prior written consent for study inclusion and were positively genotyped for HLA-DRB1\*04:01 carrier status by the Institute of Transfusion Medicine and Immunohematology, German Red Cross Blood Service Baden-Württemberg-

Hessen, Goethe University Hospital, Frankfurt. The final study population consisted of healthy blood donors (n = 20; recruited from the above mentioned Institute of the German Red Cross Blood Service in Frankfurt) and patients with RA (n = 55). The investigated RA patients (71.9% female, 21.1% male) were recruited from a cohort of RA patients treated in the outpatient clinic of the Division of Rheumatology of the Goethe University Hospital in Frankfurt, Germany. Only patients who gave their informed consent were included in the study. All patients fulfilled the 1987 revised classification criteria for (RA) of the American College of Rheumatology.[3] Ninety percent of the RA patients were positive for anti-citrullinated protein antibody and/or rheumatoid factor. All patients had well-established RA with a disease duration of >3 years and were receiving treatment with disease-modifying antirheumatic drugs [methotrexate (MTX): 69.1%, leflunomide: 9.1%, TNF-blocking agents (in monotherapy or combination with MTX): 40%]. The prednisolone comedication was 5 mg/day p.o. or less at the timepoint of study assessments. Patients' mean DAS28CRP was in the low disease activity range ( $2.88 \pm 0.32$ ). Ethical approval was obtained by the institutional review board of the University Hospital Frankfurt.

### **Analysis of Col2-reactive in vitro expanded T cells**

Our studies aimed at the characterization of TCR with DRB1\*04:01-restricted recognition of Col2 259-273. For this purpose, CD154<sup>+</sup> / CD4<sup>+</sup> T cells were sorted by flow cytometry following PBMC stimulation with the gal<sub>264</sub>Col2<sub>259-273</sub> peptide. The FACS-sorted CD154<sup>+</sup> / CD4<sup>+</sup> T cells were subsequently cultured for 30 days in the medium and supplemented with IL-2 (0.1 ng/mL) every four days in the presence αCD2, αCD3 and αCD28 beads contained in a commercial kit for T cell expansion according to the manufacturer's instructions (T Cell Activation/Expansion Kit, Miltenyi). Subsequently, TCR specificity of the cells was analyzed by flow cytometry upon staining with DRB1\*04:01/gal<sub>264</sub>Col2<sub>259-273</sub> tetramers followed by

single-cell sorting into a 96-hole PCR plate using a FACS Aria flow cytometry system (BD) and storage at  $-80^{\circ}\text{C}$  for subsequent TCR  $V\alpha$  and  $V\beta$  gene amplification by PCR.

### **Single-cell PCR of gene segments encoding the variable region of the TCR**

mRNA of the TCR  $\alpha$ - and  $\beta$ -chains from single-sorted cells was transcribed into cDNA for 30 min at  $50^{\circ}\text{C}$  by using a one-step RT-PCR kit (Qiagen, Hilden, Germany) and constant region-specific RT primers at  $0.625\ \mu\text{M}$  each.[4] Then primers for the simultaneous preamplification of  $\alpha$ - and  $\beta$ -chains were added. Two rounds of PCR were required for amplification of the variable region gene segments. A pool of specific 5' primers covering with their distinct specificities the diverse gene segment families of the variable ( $V\alpha$  or  $V\beta$ ) regions of human TCRs were applied for the initial round of amplification. Thus, all 24  $V\alpha$  region-specific 5' primers were used in combination with a 3' primer ( $C\alpha$ -rev-out) in the constant region for  $V\alpha$  gene amplification.[4] The PCR reaction was composed of  $3.5\ \mu\text{l}$  of cDNA template,  $2\ \mu\text{l}$  dNTP ( $10\text{mM}$ ),  $2\ \mu\text{l}$  Primer Mix ( $2.5\ \mu\text{M}$ ),  $4\ \mu\text{l}$  Puffer 3- (Merck),  $4\ \mu\text{l}$  MgCl ( $25\ \text{mM}$ ), and  $1\ \mu\text{l}$  Polymerase Expand ( $3\text{U}$ ) with water added to a final volume of  $50\ \mu\text{l}$ . The run off conditions were  $94^{\circ}\text{C}$  for 30 sec,  $55^{\circ}\text{C}$  for 30 sec, and  $72^{\circ}\text{C}$  for 55 sec (50 cycles).

In the 2nd round, parallel amplifications were performed with newly compiled pools of 7 to 8  $V\alpha$  gene-specific 5' primers each mixed with a 3' primer ( $C\alpha$ -rev-in) located in the constant region.[5] The TCR  $\beta$ -PCR products were amplified accordingly using specific 5' primers for 9  $V\beta$  regions and the constant 3' primer ( $C\beta$ -in-rev).[6] All forward primers and the C-specific reverse primer were nested relative to the outer primers used in the preamplification reaction. The second PCR round was composed of  $3.5\ \mu\text{l}$  template of the first round,  $0.5\ \mu\text{l}$  dNTP ( $10\text{mM}$ ),  $2\ \mu\text{l}$  5' primer ( $2.5\ \mu\text{M}$ ),  $2\ \mu\text{l}$  3' primer ( $2.5\ \mu\text{M}$ ),  $5\ \mu\text{l}$  Puffer 2+ (Merck),  $1\ \mu\text{l}$  MgCl ( $25\ \text{mM}$ ), and  $0.3\ \mu\text{l}$  Polymerase Expand ( $1\text{U}$ ), with water added to a final volume of  $50\ \mu\text{l}$ . The run off conditions were  $94^{\circ}\text{C}$  for 30 sec,  $58^{\circ}\text{C}$  for 30 sec, and  $72^{\circ}\text{C}$

for 45 sec (50 cycles). Sequencing of amplified cDNA was carried out by a service provider (Seqlab-Microsynth, Germany) using the dideoxynucleotide chain termination method. Obtained variable region TCR sequences were analyzed by the IMGT /V-Quest program.[7, 8]

### **Lentiviral transfection of TCR $\alpha$ and $\beta$ chain cDNA into a Jurkat 76 cell line**

The full-length cDNAs encoding the TCR  $\alpha$  and  $\beta$  chains were cloned into a SIEW vector (expression construct) using the SacII and PasI restriction cleavage sites. The vector construct contains a WPRE (Woodchuck posttranscriptional regulatory element) as expression enhancer, a T2A (Thosea asigna virus 2A) peptide sequence, and an IRES (ribosomal entry point) element to ensure continuous transcription as well as an eGFP (Green fluorescent protein) encoding sequence to facilitate control of transduction efficiency. The lentiviral vectors for Jurkat transduction were produced by HEK293 cells. For this purpose, the HEK293 cells were cotransfected with the viral transfer vector (15  $\mu$ g), a packaging plasmid (gag/pol, Plasmid M334, 10  $\mu$ g) and an envelope plasmid (env, Plasmid VSV-G, 5  $\mu$ g) using polyethyleneimine (PEI) derivative Jet-Pei® (PolyPlus) as transfection reagent. The infectious particles released into medium (DMEM containing 10% fetal bovine serum and 1% penicillin-streptomycin) during a 72 h incubation period were harvested and used for subsequent transduction of Jurkat 76 cells deficient in endogenous TCR  $\alpha$  and  $\beta$  chains (kindly provided by TRON gGmbH, Mainz). The Jurkat cells were seeded in a 24-well plate ( $1 \times 10^5$  cells/500  $\mu$ l) and co-incubated with 500  $\mu$ l of the self-produced virus particles for 4 days. Transduction efficacy was controlled by GFP expression and specific tetramer staining using cytofluorometry.

### **Functional analysis of Jurkat 76 cells upon lentiviral TCR gene transfer**

The transduced Jurkat cells were stimulated with different recombinant MHCII/peptide complexes (5 µg/ml) in a 24-well plate at a density of  $1 \times 10^5$  cells/mL at 37°C for 24 h. The TCR-induced response of IL-2 release was determined in the cell supernatants using a commercial sandwich enzyme-linked immunosorbent assay (ELISA) according to the manufacturer's instructions (ELISA Max™ human IL-2 Delux Set, Biologend, San Diego, USA).

### **TCR mRNA design and in vitro transcription**

The full-length cDNAs encoding either the TCR  $\alpha$  or  $\beta$  chain were synthesized and cloned into a pMA vector by GeneArt Gene Synthesis (Thermo Fisher Scientific) using AscI and KpnI as restriction cleavage sites. The constructs included an enhanced T7 promoter, the Kozak sequence, the respective  $\alpha$  or  $\beta$  chain including its signal peptide, two stop codons, a four-fold repeat of the VEEV (Venezuelan equine encephalitis virus) 3'UTR [9] and a 40-A PolyA tail. The constant region of the chains had been mutated to improve alpha and beta chain dimerization and its stabilization by introducing an additional disulfide bond (alpha constant region: T48C, beta constant region: S57C).[10]

For the subsequent in vitro production of corresponding mRNAs, restriction digestion of 2 µg plasmid DNA was performed with KpnI (Thermo Fisher Scientific, FD0524) for at least one hour at 37°C and terminated by heat inactivation at 80°C for 5 min. The linearized plasmids served as templates for the separate in vitro transcription of the respective  $\alpha$ - and  $\beta$ -TCR chains using the HiScribe™ T7 ARCA mRNA Kit (NEB, E2065S); mRNA purification was achieved via application of the Monarch® RNA Cleanup Kit (NEB, T2050S).

### **TCR $\alpha$ and $\beta$ chain mRNA electroporation into Jurkat cell lines**

10  $\mu$ g mRNA of each TCR chain was mixed for cell electroporation with the Neon<sup>TM</sup> Transfection System (Thermo Fisher Scientific). 5 x 10<sup>6</sup> Jurkat-Lucia<sup>TM</sup> nuclear factor of activated T cells (NFAT) cells (invivogen, jktl-nfat) or Jurkat 76 cells in 100  $\mu$ l R buffer were added to the prepared mRNA, taken up in 100  $\mu$ l Neon<sup>TM</sup> tips (Thermo Fisher Scientific, MPK10096) and treated with three 1500 V, 10 ms square pulses. After electroporation, the cells were transferred to 10 mL of Iscove's Modified Dulbecco's Medium (IMDM) containing 10% fetal bovine serum (FBS). For a negative control cells were treated under identical conditions but without any addition of mRNA. Effectiveness of mRNA transfection was controlled by flow cytometry of TCR-stained Jurkat 76 cells that had been electroporated with or without a TCR mRNA additive. Cell surface staining was done 24 hours after electroporation using an antibody against the constant region of the human TCR beta chain.

### **Antigen-presenting cells (APC)/Quanti-Luc Assay: Functional analysis of Jurkat-Lucia<sup>TM</sup> NFAT cells upon electroporation with TCR mRNA and co-culture with APCs presenting gal<sub>264</sub>Col<sub>259-273</sub>, nCol<sub>259-273</sub> or CLIP peptides**

Jurkat-Lucia<sup>TM</sup> NFAT cells were electroporated with mRNA of the  $\alpha$  and  $\beta$  chain of TCR #16 for functional analyses in an APC assay. For this purpose, human APCs were obtained from PBMCs of a healthy DRB1\*04:01-positive donor via CD3 depletion by magnetic-activated cell sorting (MACS) sorting (Miltenyi) and stored frozen until use. Two days prior to experimental use the thawed APCs were taken into culture for recovery in TexMACS<sup>TM</sup> Medium (Miltenyi, 130-097-196) with 1% penicillin-streptomycin. 1 x 10<sup>4</sup> cells were seeded in 100  $\mu$ L medium per well in a 96-well plate. Five hours prior to co-culture with the freshly electroporated Jurkat-Lucia<sup>TM</sup> NFAT cells, the APCs were preincubated with peptides (0.1  $\mu$ g/ml, 10  $\mu$ g/ml of gal<sub>264</sub>Col<sub>259-273</sub>, nCol<sub>259-273</sub> or class II-associated invariant chain peptide CLIP<sub>85-103</sub> [PVSKMRMATPLLMQALPM]) to ensure peptide loading of the MHCII molecules on

their cell surface. Then the APCs were washed with PBS, fixed with 1% PFA for 4 min, and then again washed twice. For the co-culture the Jurkat-Lucia™ NFAT cells were added to the APCs in 100 µl Quanti-Luc Test Medium (IMDM, 10% FBS, 1% penicillin-streptomycin) and cultured for 36 hours at 37°C. As a positive control for TCR-dependent cell activation, Jurkat-Lucia™ NFAT were stimulated with 10 µg/ml ConA (Concanavalin A; Sigma Aldrich, C5275).

The supernatant was tested for luciferase secretion upon TCR activation via QUANTI-Luc™ (InvivoGen, rep-qlc1) luminescence detection. A reduced version of the detection assay was used as only 10 µl supernatant was mixed with 25 µl oQUANTI-Luc™ substrate before luminescence was detected for a duration of 1 second using the Mithras LB940 plate reader time (Berthold Technologies, Bad Wildbad, Germany).

### **Crystallization procedures**

For crystallization experiments, the DRB1\*04:01-peptide complexes were prepared as described above and digested by Tobacco Etch Virus (TEV) enzyme to remove Fos-Jun motif and His-tag. The remaining part for crystallization was purified with an additional ion exchange chromatographic step. Briefly, the digested protein was loaded onto a Mono QTM 10/100 GL column (GE Healthcare) equilibrated with 10 mM Tris-HCl (pH 7.5), 10 mM NaCl, and eluted with a linear gradient of increasing NaCl concentration. The DRB1\*04:01-peptide complex was eluted, concentrated to 6 mg/mL, and stored at -80°C for further use.

Crystals of the protein DRB1\*04:01-peptide complexes were grown by the sitting drop vapor diffusion method. Sitting drops containing equal volumes of the protein and reservoir solutions were equilibrated at room temperature against the reservoir solution. The crystals were transferred to a cryo-protection solution prior to data collection.

Screening for crystallization conditions was performed using commercially available sparse-matrix screens in a sitting-drop vapor diffusion mode and nanodrop setup at 293 K. The sitting drops contained equal volumes of the protein and reservoir solutions. Obtained crystals were transferred to a cryo-protection solution prior to data collection.

The crystals used for data collection were grown and cryo-protected as follows:

DRB1\*04:01+ hCol2<sub>259-273</sub>: The sitting drop was pipetted from 0.2  $\mu$ l protein solution (6 mg/mL in 10 mM Tris pH 7.4, 20 mM NaCl) and 0.2  $\mu$ l reservoir solution (0.1M MMT buffer pH 5.0, 25 % (w/v) PEG 1500). The crystal was cryo-protected by brief soaking in 17% (w/v) 0.1M MMT buffer pH 5.0, 25 % (w/v) PEG 1500, 25% (w/v) glycerol.

DRB1\*04:01+ mutCol2<sub>259-273</sub>: The sitting drop was pipetted from 0.2  $\mu$ l protein solution (6 mg/mL in 10 mM Tris pH 7.4, 20 mM NaCl) and 0.2  $\mu$ l reservoir solution (0.1 M MIB buffer pH 4.0, 25 % [w/v] PEG 1500). The crystal was cryo-protected by brief soaking in 17% (w/v) 0.1 M MIB buffer pH 4.0, 25 % (w/v) PEG 1500, 25% (w/v) glycerol.

DRB1\*04:01+ cit-CILP<sub>982-996</sub>: The sitting drop was pipetted from 0.15  $\mu$ l protein solution (6 mg/mL in 10 mM Tris pH 7.4, 20 mM NaCl) and 0.15  $\mu$ l reservoir solution (0.1M sodium acetate trihydrate pH 5.5, 0.2M lithium chloride, 18% [w/v] PEG6000). The harvested crystal was cryo-protected by soaking in 0.1M sodium acetate trihydrate pH 5.5, 0.2M lithium chloride, 18% (w/v) PEG6000, 25% (w/v) glycerol.

DRB1\*04:01+ HSP70<sub>289-306</sub>: The sitting drop was pipetted from 0.15  $\mu$ l protein solution (6 mg/mL in 10 mM Tris pH 7.4, 20 mM NaCl) and 0.15  $\mu$ l reservoir solution (0.03 M of each divalent cation (Magnesium chloride hexahydrate, Calcium chloride dihydrate), 12.5% (w/v) PEG 1000, 12.5% (w/v) PEG 3350, 12.5% (v/v) MPD, 0.1 M MOPS/HEPES-Na pH 7.5). The harvested crystal was cryo-protected by soaking in 0.03 M of each divalent cation (12.5% [w/v] PEG 1000, 12.5% [w/v] PEG 3350, 12.5% [v/v] MPD), 0.1 M MOPS/HEPES-Na pH 7.5, 25% (w/v) glycerol.

### **X-ray diffraction data collection and structure determination**

Diffraction data were collected at the beamlines and with the statistics given in Table S1. The images were processed using XIA2,[11-13] and scaled by AIMLESS [14] from the CCP4 program suite.[13]

The structures of peptide-DRB1\*04:01 complexes were determined by molecular replacement using PHASER.[16] Iterative cycles of the manual model building using COOT [17] and TLS and restrained refinement with Phenix or REFMAC5 [18] were used until R-factors converged. Refinement statistics are given in Table S1. About 5% of the reflections were randomly selected and set aside for unbiased cross-validation (calculation of  $R_{\text{free}}$ ). All final models have good stereochemistry, with >96% of the residues in the most favored regions of the Ramachandran plot (Table S1). Figures were prepared with PyMol.[19] The crystallographic coordinates and structure factors have been deposited in the Protein Data Bank with the accession codes listed in Table S1.

### **Molecular model generation**

The geometry of the MHCII/peptide complex was directly taken from the X-ray structure presented in this work. The human  $\alpha/\beta$  TCR #16 was generated by homology using the SWISS-MODEL web service,[20, 21] according to the published X-ray structure of a human TCR, co-crystallized with a MHCII/influenza antigen peptide complex (protein databank entry 1J8H, accessible via [www.pdb.org](http://www.pdb.org)). The quaternary structure of the final complex was generated by fitting the individual units on the X-ray structure 1J8H.

### **Molecular dynamics simulations**

To investigate the dynamic behavior and properties of the modeled systems, we performed extensive molecular dynamics simulations using the AMBER18 software package.[22, 23] Parameters for the non-standard residues 5-hydroxylysine and galactosylated 5-hydroxylysine were kindly provided by Anna Linusson, University of Umeå, Sweden. After geometry optimization to remove unfavorable steric clashes, both systems (K264 and galK264) were simulated in aqueous environment for a total time of 950 ns. All graphical representations of protein structures were generated with UCSF Chimera.[24, 25]

### **Statistical analyses**

Statistical analyses were performed by GraphPAD Prism 5 software. Data were expressed as the mean  $\pm$  SEM. Statistical significance for flow cytometry assessments of differences in human antigen-specific T cells in PBMC was determined using the Mann-Whitney test. *P* values less than 0.05 were considered significant.

**Figure S1** DRB1\*04:01 in complex with several antigenic peptides. The peptide-binding groove of the HLA-DR molecule is shown in cartoon representation with the  $\alpha$ -chain colored in dark pink and the  $\beta$ -chain colored in blue. The peptide is shown as sticks.

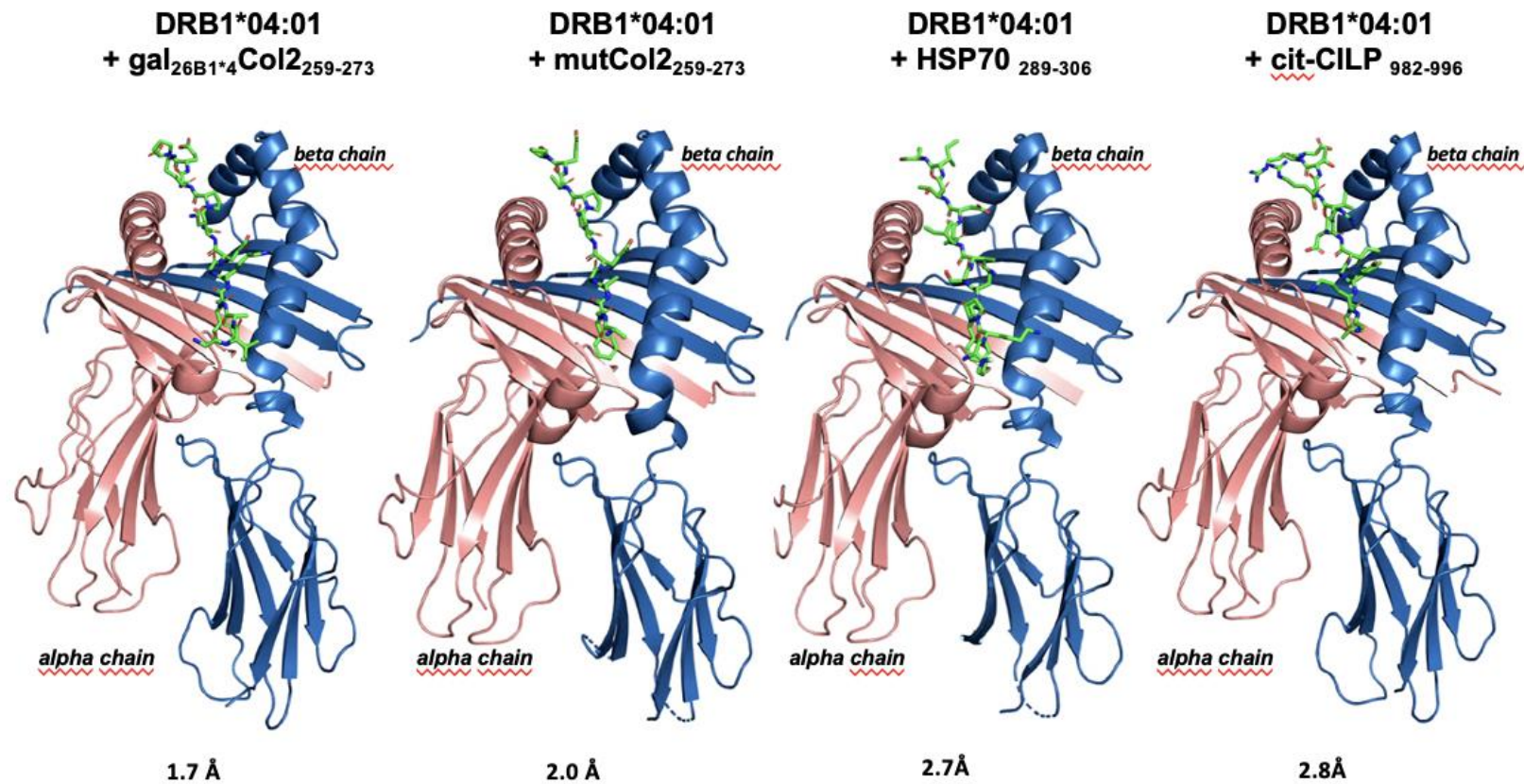


**Figure S2** Superimposition of the mutated and gal<sub>264</sub> wild type peptide of Col2<sub>259-273</sub> on DRB1\*04:01.

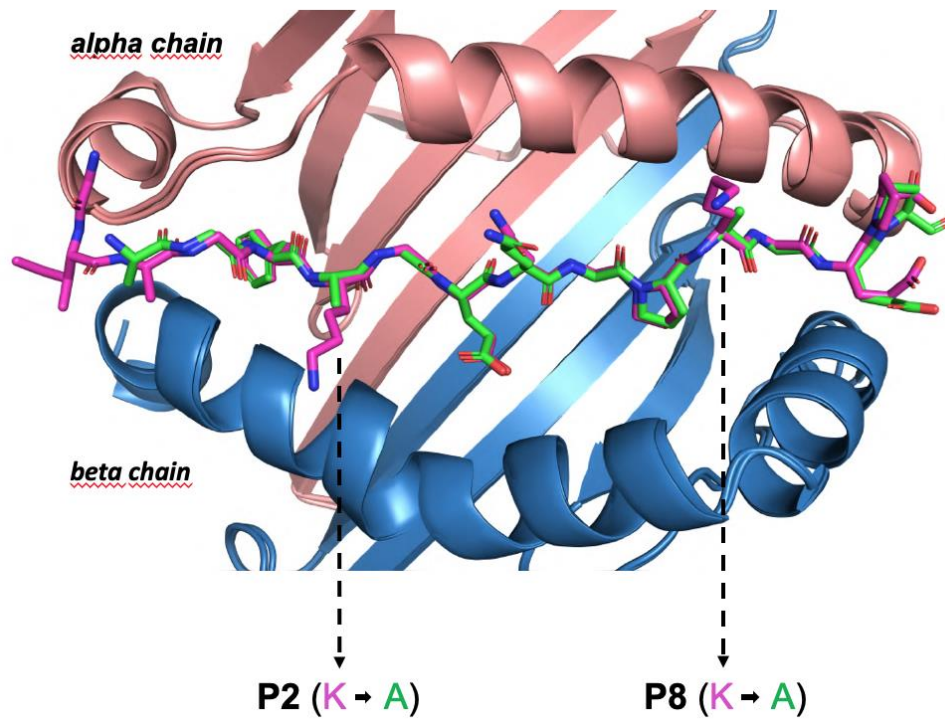


**Figure S3** cDNA sequence of the human galCol2-specific TCR #16. V-gene analysis was performed using the v-quest tool [7] IMGT information system.

**TRAV8-4\*01 / TRAJ8\*01**

**α-chain:**

FR1 CDR1 FR2

gccacgtctgtgacacagctgtggcagccacgttcagtgctgaaggtgcccctggctgctgagatgcaactactct agcagcgtgccaccttac ctgttttggtaoigtccagtacccccaaccaggagctgagctgctgctgaag

CDR2 FR3

tacacatctgccgccacactggtc aagggtcatcaatggctctgagggcogagttcaagaagtccgagacaagcttccacctgacaagcctagcctcacaatgtccgacgcccgagatattttgcg

CDR3 FR4

cogtgtccgatagactgaaacacggcttccagaaaactggtg ttggcaocggaaocagactgctgggltgcccctaac

**TRBV13\*01 / TRBD2\*01 / TRBJ1-6\*01**

**β-chain:**

FR1 CDR1 FR2

gccggcgtgatccagctctcctagacacctgatcaaagagaagcggagagacagccacactgaagtctaccocatt cctcggcagcacacc gtgtactgtatcagcaaggaccocggocaggatcctcagttcctgatcagc

CDR2 FR3

ttctaogagaagatgcag agcgecaagggcagcatccccgatagattcagcgcocagcagttcagogaattaccacagcagctgaacatgagcagcctggaaactggogalagocccctgactttigt

CDR3 FR4

gocagctctctggccggcaacagccctctgcac ttggcaatggcaaccagaactgaoccgigaacc

**Figure S4** Amino acid sequence of the human galCol2 specific TCR #16. Sequence in single letter code obtained by translation of the cDNA sequence depicted in Figure S3.

**TRAV8-4\*01 / TRAJ8\*01**

V-Gen α-chain:

|                                    |                |                |           |
|------------------------------------|----------------|----------------|-----------|
| FR1                                | CDR1           | FR2            | CDR2      |
| AQSVTQLGSHVSVSEGalVLLRCNYS         | SSVPPYLFW      | YVQYPNQGLQLLLK | Y TSAATLV |
| FR3                                | CDR3           | FR4            |           |
| KGINGFEAEFKKSETSFHLTKPSAHMSDAAEYFC | AVSDRLNTGFQKLV | FGTGTRLLVSPN   |           |

**TRBV13\*01 / TRBD2\*01 / TRBJ1-6\*01**

V-Gen β-chain:

|                                       |             |                  |        |
|---------------------------------------|-------------|------------------|--------|
| FR1                                   | CDR1        | FR2              | CDR2   |
| AGVIQSPRHLIKEKRETATLKCYP              | PRHDT       | VYWYQQGPGQDPQLIS | FYEKMQ |
| FR3                                   | CDR3        | FR4              |        |
| SDKGSIPDRFSAQQFSDYHSELNMSSLELGDSALYFC | ASSLAGNSPLH | FGNGTRLLTVI      |        |

**Figure S5** Binding of DRB1\*04:01 tetramers to TCR-deficient Jurkat cells and induction of IL-2 after gene transfer of the cloned alpha and beta chain of TCR #21 or TCR # 22.

A) Flow cytometric analysis of binding of DRB1\*04:01/gal<sub>264</sub>Col<sub>2259-273</sub> tetramers to TCR-deficient Jurkat 76 cells after gene transfer of the cloned  $\alpha$  and  $\beta$  chains of either TCR #21 or #22. Transduction of a TCR-deficient Jurkat 76 cell line was performed with a lentiviral vector either encoding the  $\alpha$  and  $\beta$  chains of TCR #21 (TRAV9-2/TRAJ20; TRBV14/TRBD2/TRBJ1-5) or TCR #22 (TRAV12-3/TRAJ43; TRBV13/TRBD2/TRBJ1-6). Each of the cDNAs encoding TCR #21 and #22 were cloned from single T cells derived from two different DRB1\*04:01-positive RA patients. The respective T cells were selected from an *in vitro* expanded pool of gal<sub>264</sub>Col<sub>2259-273</sub> peptide-reactive CD4<sup>+</sup> T lymphocytes by specific DRB1\*04:01/gal<sub>264</sub>Col<sub>2259-273</sub> tetramer staining following the same protocol described for TCR #16. Transduced Jurkat cells were stained with a dead/live marker and DRB1\*04:01/peptide tetramers conjugated with two different fluorophores (PE and APC). Flow cytometric analysis revealed tetramer-specific cells in the live double-positive stained subpopulation. A biotin-streptavidin complex without a specific peptide conjugate served as negative control. (B) Induction of specific IL-2 responses in transduced Jurkat 76 cells expressing either the human TCR receptor #21 or #22 by stimulation with DRB1\*04:01/Col<sub>2259-273</sub> peptide complexes. Transduced Jurkat cells were incubated with soluble DRB1\*04:01/peptide complexes for 24 h. Specific activation of cells via the TCR was measured by induced IL-2 release specific capture ELISA. Unstimulated cells served as a negative control. The MHCII restriction of TCR was performed by stimulation with the murine Aq/gal<sub>264</sub>Col<sub>2</sub> peptide complex. Bars indicate mean values, lines indicate standard deviation, and dots represent separate experiments.

Aq, murine MHCII allele; APC, allophycocyanin; ELISA, enzyme-linked immunosorbent assay; HA, influenza hemagglutinin 306-318; IL, interleukin; ns, not significant; PE, phycoerythrin; TCR, T-cell receptor.

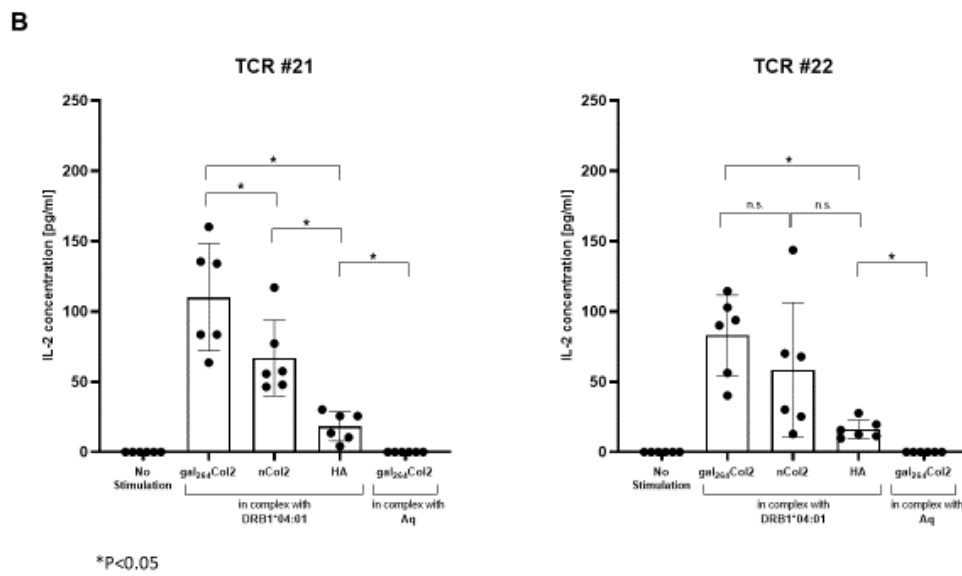
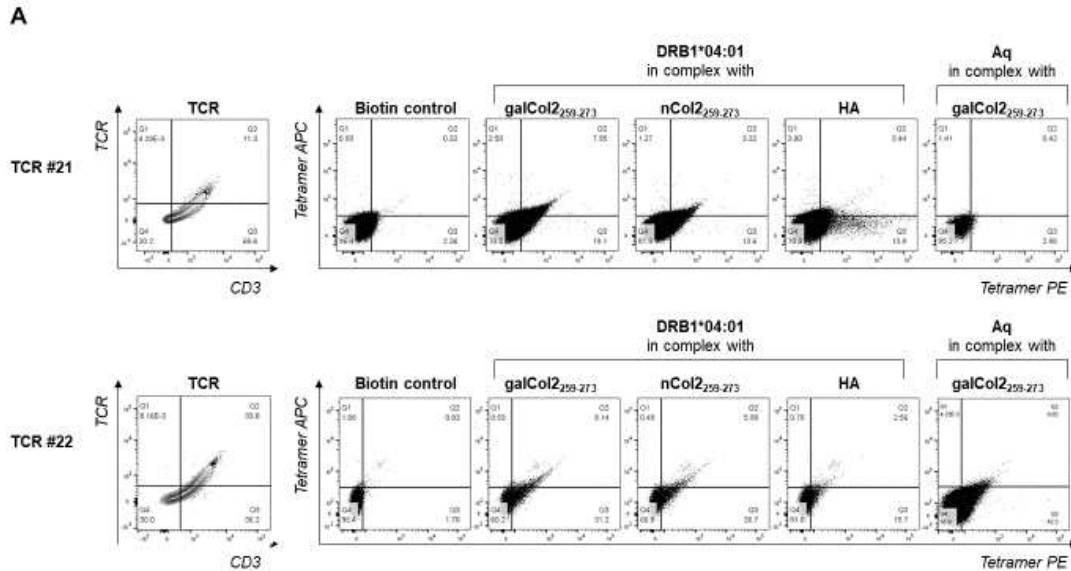


**Figure S6** Functional analysis of Jurkat-Lucia™ NFAT cells transiently expressing the TCR #16 upon mRNA electroporation to specifically recognize DRB1\*04:01/ peptide complexes on the surface of fixed APCs preloaded with gal<sub>264</sub>Col<sub>259-273</sub>, nCol<sub>259-273</sub> or CLIP peptides under co-culture conditions. The upper left panel is a graphical abstract of the applied methodology described in detail in the Materials and Methods section. \*Antigen presenting cells (APC): CD3 depleted PBMC from a DRB1\*04:01 healthy donor and splenocytes from DRA1/DRB1\*04:01 knock-in-mouse. §Jurkat-Lucia™ NFAT cells were electroporated with mRNA of the alpha and beta chain of TCR #16 for functional analysis in an APC assay.

A) TCR deficient Jurkat-76 cells were electroporated with the alpha and beta chain of TCR #16 under identical conditions as the Jurkat-Lucia™ NFAT cells (applied to experiments of which the results are shown in B and C). Sham electroporated controls and TCR# 16 mRNA transfected cells were stained with a dead/live marker and an anti-human TCR antibody conjugated with the fluorophore PE. Subsequent flowcytometric analysis reveals a high percentage of anti-human TCR positive cells only in the live subpopulation of TCR#16 mRNA transfected cells (dot blot presentation in the right panel) but not in the respective control subpopulation of cells electroporated without a mRNA additive (left panel) thereby providing evidence for efficient electroporation conditions of TCR#16 mRNA.

Results of luciferase induction in Jurkat-Lucia™ NFAT cells either sham electroporated (no mRNA) or transfected with alpha and beta chain mRNA of TCR#16 during coculture with peptide pulsed APCs. The measured arbitrary units (AU) of luminescence resulting from the conversion of the luciferase substrate reflect the released catalytic activity that depends on TCR mediated upregulation of NFAT transcriptional activity by the specific recognition of the

different peptides in a DRB1\*04:01 context on the surface of the fixed APCs: A human APC preparation was obtained from CD3 depleted PBMCs of a healthy human donor (B) and murine splenocytes derived from a Col2 immunized arthritic DRB1\*04:01 knock-in mouse served as APCs in studies of which the results are shown in C). The different peptides and their applied concentrations are indicated in the Figure.

The results provide clear evidence, that presentation of the glycosylated Col2 peptide in a DRB1\*04:01 context on fixed APC of both murine as well as human origin results in a specific recognition by TCR#16 mRNA transfected Jurkat-Lucia™ NFAT cells resulting in a stronger NFAT activation compared to the naked Col2 peptide. The CLIP control peptide did not activate the TCR mRNA electroporated Jurkat reporter cells under identical experimental conditions and the sham transfected Jurkat-Lucia™ NFAT cells did not exhibit any induction of luciferase activity via its endogenous TCR.

APC, antigen-presenting cell; CLIP, class II-associated invariant chain peptide; ConA, concanavalin A; FCS, forward scatter; TCR, T-cell receptor

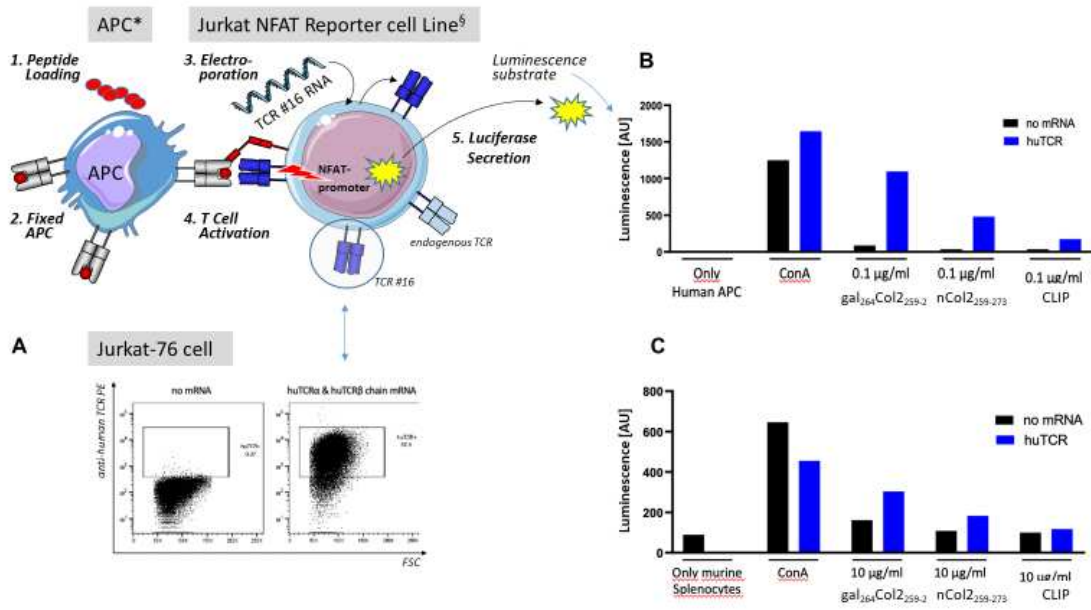
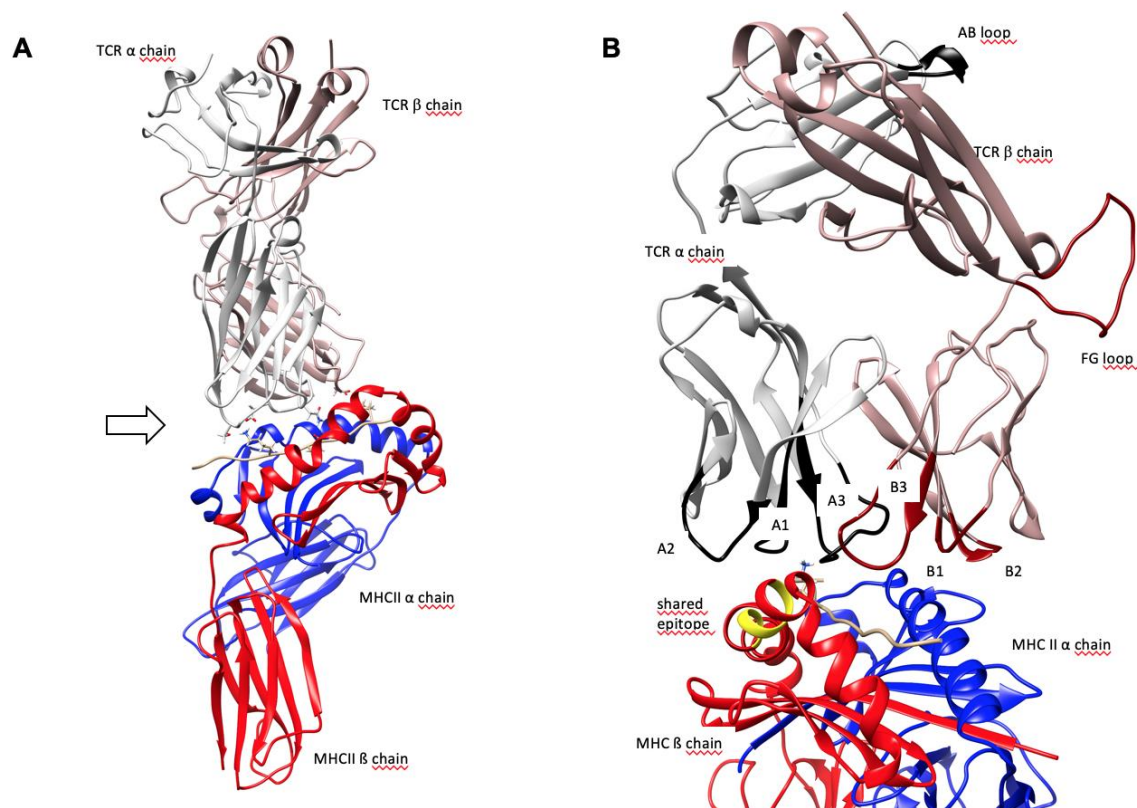


**Figure S7** Molecular model of the three-dimensional structure of the multicomponent system consisting of the DRB1\*04:01/Col2 peptide/TCR complex after geometry optimization. The Col2<sub>259-273</sub> peptide is located between the  $\alpha$ 1- and  $\beta$ 1-helices of DRB1\*04:01 and is being presented to the human TCR #16 that is approaching from above. (A) Side view at lower resolution. The arrow indicates the perspective of the enlarged image section shown in (B). (B) The focus is on the Col2 peptide orientation in the DRB1\*04:01-binding groove and its contact with the domains A3 and B1 of the TCR variable region. Some functional domains are highlighted by different colors: the so-called “shared-epitope“ region of the DRB1\*04:01  $\beta$ -chain (residues:70-74, yellow), the constant regions of TCR #16: the C $\alpha$  AB loop (black) and the C $\beta$  FG loop (salmon red). MHC, major histocompatibility complex; TCR, T-cell receptor.



**Supplemental Table S1. Data collection and refinement statistics.**

| Parameter                                  | DRB1*04:01-GalCol2 <sub>259-273</sub>      | DRB1*04:01-mutCol2 <sub>259-273</sub> | DRB1*04:01-citCILP <sub>982-996</sub> | DRB1*04:01-HSP70 <sub>289-306</sub> |
|--|--|---------------------------------------|---------------------------------------|-------------------------------------|
| <b>PDB ID</b>                              | 7NZE                                       | 7NZF                                  | 7NZH                                  | 7O00                                |
| <b>Beam line</b>                           | Diamond I04                                | Diamond I03                           | BessyII                               | Diamond I03                         |
| <b>Resolution range(Å)</b>                 | 46.96 - 2.05<br>(2.12 - 2.05) <sup>#</sup> | 36.92 - 1.90<br>(1.97 - 1.90)         | 49.65 - 2.83<br>(2.93 - 2.83)         | 69.60 - 2.24<br>(2.32 - 2.24)       |
| <b>Space group</b>                         | C2   | P3 <sub>2</sub> 21                    | C222 <sub>1</sub>                     | P4 <sub>3</sub> 22                  |
| <b>Unit cell<br/>a, b, c (Å)<br/>β (°)</b> | 122.4 71.8 125.7<br>111.3                  | 71.4 71.4 138.0                       | 97.3 112.2 213.0                      | 76.2 76.2 170.6                     |
| <b>Total reflections</b>                   | 436701 (43659)                             | 359241 (36561)                        | 370272 (34778)                        | 646346 (65126)                      |
| <b>Unique reflections</b>                  | 63751 (6260)                               | 32445 (3183)                          | 27761 (2678)                          | 25036 (2446)                        |
| <b>Multiplicity</b>                        | 6.9 (6.9)                                  | 11.1 (11.5)                           | 13.3 (13.0)                           | 25.8 (26.6)                         |
| <b>Completeness (%)</b>                    | 97.8 (98.7)                                | 98.4 (97.9)                           | 98.5 (96.1)                           | 99.9 (99.9)                         |
| <b>Mean I/sigma(I)</b>                     | 14.0 (1.9)                                 | 18.2 (3.4)                            | 14.3 (1.5)                            | 12.2 (0.9)                          |
| <b>Wilson B-factor</b>                     | 35.5                                       | 26.8                                  | 76.3                                  | 21.7                                |
| <b>R-merge</b>                             | 0.075 (0.879)                              | 0.090 (0.756)                         | 0.157 (1.872)                         | 0.244 (3.132)                       |
| <b>R-meas</b>                              | 0.081 (0.950)                              | 0.09446 (0.7909)                      | 0.163 (1.949)                         | 0.2489 (3.193)                      |
| <b>R-pim</b>                               | 0.031 (0.359)                              | 0.028 (0.231)                         | 0.044 (0.532)                         | 0.049 (0.616)                       |
| <b>CC1/2</b>                               | 0.999 (0.867)                              | 0.999 (0.889)                         | 0.998 (0.51)                          | 0.999 (0.741)                       |
| <b>CC*</b>                                 | 1 (0.964)                                  | 1 (0.97)                              | 1 (0.822)                             | 1 (0.923)                           |
| <b>Refinement</b>                          |  |                                       |                                       |                                     |
| <b>R-work</b>                              | 0.2517 (0.3820)                            | 0.2686 (0.3234)                       | 0.2672 (0.3798)                       | 0.2444 (0.3563)                     |
| <b>R-free</b>                              | 0.2871 (0.4337)                            | 0.3064 (0.3546)                       | 0.3092 (0.3530)                       | 0.2867 (0.3744)                     |
| <b>Number of non-hydrogen atoms</b>        | 6780                                       | 3221                                  | 6394                                  | 3230                                |
| <b>Protein</b>                             | 6367                                       | 3022                                  | 6296                                  | 3028                                |

| Parameter                                | DRB1*04:01-<br>GalCol2 <sub>259-273</sub> | DRB1*04:01-<br>mutCol2 <sub>259-273</sub> | DRB1*04:01-<br>citCILP <sub>982-996</sub> | DRB1*04:01-<br>HSP70 <sub>289-306</sub> |
|--|---|---|---|---|
| Ligands                                  | 66  | 28  | 98  | 28                                      |
| Solvent                                  | 347                                       | 171                                       | 0   | 174                                     |
| Average B-factor (all atoms)             | 24.1                                      | 19.4                                      | 52.5                                      | 31.4                                    |
| RMSD (bonds, Å)                          | 0.010                                     | 0.010                                     | 0.009                                     | 0.014                                   |
| RMSD (angles, °)                         | 1.40                                      | 1.39                                      | 1.39                                      | 1.95                                    |
| Residues (%) in Ramachandran plot region |   |   |   |   |
| Favored                                  | 98.15                                     | 97.22                                     | 96.75                                     | 97.49                                   |
| Allowed                                  | 1.85                                      | 1.94                                      | 2.98                                      | 2.51                                    |
| Outliers                                 | 0.00                                      | 0.83                                      | 0.27                                      | 0.00                                    |

#Statistics for the highest-resolution shell are shown in parentheses.

**SUPPLEMENTARY MATERIAL REFERENCES**

1. Holm B, Broddefalk J, Flodell S, Wellner E, *et al.* An improved synthesis of a galactosylated hydroxylysine building block and its use in solid-phase glycopeptide synthesis. *Tetrahedron* 2000;56:1579-86.
2. Gauthier L, Smith KJ, Pyrdol J, *et al.* Expression and crystallization of the complex of HLA-DR2 (DRA, DRB1\*1501) and an immunodominant peptide of human myelin basic protein. *Proc Natl Acad Sci U S A* 1998;95:11828-33.
3. Arnett FC, Edworthy SM, Bloch DA, *et al.* The American Rheumatism Association 1987 revised criteria for the classification of rheumatoid arthritis. *Arthritis Rheum* 1988;31:315-24.
4. Seitz S, Schneider CK, Malotka J, *et al.* Reconstitution of paired T cell receptor  $\alpha$ - and  $\beta$ -chains from microdissected single cells of human inflammatory tissues. *Proc Natl Acad Sci U S A* 2006;103:12057-62.
5. Han A, Glanville J, Hansmann L, *et al.* Linking T-cell receptor sequence to functional phenotype at the single-cell level. *Nat Biotechnol* 2014;32:684–92.
6. Kim SM, Bhonsle L, Besgen P, *et al.* Analysis of the paired TCR  $\alpha$ - and  $\beta$ -chains of single human T cells. *PLoS One* 2012;7:e37338.
7. Brochet X, Lefranc MP, Giudicelli V. IMGT/V-QUEST: the highly customized and integrated system for IG and TR standardized V-J and V-D-J sequence analysis. *Nucl Acids Res* 2008;36:W503-508.
8. The International Immunogenetics Information System. Available: [www.imtg.org](http://www.imtg.org). Accessed March 2021.
9. Hayashi T, Lamba DA, Slowik A *et al.* A method for stabilizing RNA for transfection that allows control of expression duration. *Dev Dyn.* 2010;239:2034-40.

10. Cohen CJ, Li YF, El-Gamil M et al. Enhanced antitumor activity of T cells engineered to express T-cell receptors with a second disulfide bond. *Cancer Res.* 2007; 67: 3898-903.
11. Winter G, Lobley CM, Prince SM. Decision making in xia2. *Acta Crystallogr D Biol Crystallogr* 2013;69:1260-73.
12. Sauter NK, Grosse-Kunstleve RW, Adams PD. Robust indexing for automatic data collection. *J Appl Crystallogr* 2004;37:399-409.
13. Evans P. Scaling and assessment of data quality. *Acta Crystallogr D Biol Crystallogr* 2006;62:72-82.
14. Evans PR, Murshudov GN. How good are my data and what is the resolution? *Acta Crystallogr D Biol Crystallogr* 2013;69:1204-14.
15. Collaborative Computational Project N. The CCP4 suite: programs for protein crystallography. *Acta Crystallogr D Biol Crystallogr* 1994;50:760-3.
16. McCoy AJ, Grosse-Kunstleve RW, Adams PD, et al. Phaser crystallographic software. *J Appl Crystallogr* 2007;40:658-74.
17. Emsley P, Lohkamp B, Scott WG, et al. Features and development of Coot. *Acta Crystallogr D Biol Crystallogr* 2010;66:486-501.
18. Murshudov GN, Vagin AA, Dodson EJ. Refinement of macromolecular structures by the maximum-likelihood method. *Acta Crystallogr D Biol Crystallogr* 1997;53:240-55.
19. The PyMOL Molecular Graphics System, Version 1.8. 2015. Schrödinger, LLC.
20. Waterhouse A, Bertoni M, Bienert S, et al. SWISS-MODEL: homology modelling of protein structures and complexes. *Nucleic Acids Res* 2018;46(W1);W296-W303.

21. Swiss Institute of Bioinformatics. SWISS-MODEL. Available: <https://swissmodel.expasy.org/>. Accessed March 2021.
22. Case DA, Ben-Shalom IY, Brozell SR, *et al.* AMBER 2018, University of California, San Francisco.
23. The Amber Home Page. Available: [www.ambermd.org](http://www.ambermd.org). Accessed March 2021.
24. Pettersen EF, Goddard TD, Huang CC, *et al.* UCSF chimera—a visualization system for exploratory research and analysis. *J Comput Chem* 2004;25:1605–12.
25. UCSF Chimera. Available: [www.cgl.ucsf.edu/chimera/](http://www.cgl.ucsf.edu/chimera/). Accessed March 2021.